Monoamine oxidase A inhibition protects the myocardium after experimental acute volume overload

Christa Huuskonen, Mari Hämäläinen[1], Timo Paavonen[2], Eeva Moilanen[1], Ari Mennander

Tampere University Heart Hospital, Cardiac Research and Tampere University; Tampere-*Finland*
[1]The Immunopharmacology Research Group, University of Tampere School of Medicine; Tampere-*Finland*
[2]Department of Pathology, Fimlab Laboratories, Tampere University Hospital, University of Tampere School of Medicine; Tampere-*Finland*

Abstract

Objective: The molecular pathway leading to myocardial cellular destruction after acute volume overload (AVO) may include monoamine oxidases. The aim of the present study was to investigate whether moclobemide (Mo), a monoamine oxidase inhibitor, protects the myocardium after AVO.
Methods: Sixty syngeneic Fischer rats underwent surgical abdominal aortocaval fistula to induce AVO. Eighteen rats were treated with Mo 10 mg/kg/day and were compared with 42 untreated rats with AVO without treatment. Myocardial recovery was analyzed using quantitative reverse transcription polymerase chain reaction for hypoxia-inducible factor 1-alpha, inducible nitric oxide synthase, interleukin 6, E-selectin, atrial natriuretic peptide (ANP), brain natriuretic peptide, vascular endothelial growth factor-alpha, matrix metalloproteinase 9, chitinase 3-like protein (YKL-40), and transforming growth factor-beta.
Results: After 3 days, the relative number of ischemic intramyocardial arteries in the left ventricle was lower in AVO treated with Mo than in without [0.04 (0.02–0.07) vs. 0.09 (0.07–0.14), point score unit]. After 1 day, ANP was lower in AVO treated with Mo than in without [0.95 (0.37–1.84) vs. 2.40 (1.33–3.09), fold changes from the baseline (FC), p=0.044], whereas after 1 and 3 days, YKL-40 was higher in AVO treated with Mo than in without [22.66 (14.05–28.83) vs. 10.06 (6.23–15.02), FC, p=0.006 and 6.03 (4.72–7.18) vs. 3.70 (2.62–5.35), FC, p=0.025].
Conclusion: Mo decreases intramyocardial arterial ischemia of the left ventricle after AVO while increases YKL-40, reflecting cellular protection during early cardiac remodeling. In the future, adding Mo may be a simple means for myocardial protection after AVO. *(Anatol J Cardiol 2019; 21: 39-45)*
Keywords: monoamine oxide A inhibition, acute volume overload, myocardial arteries, rat, YKL-40

Introduction

Acute tricuspid valve regurgitation and atrial or ventricular rupture of the cardiac septum may lead to acute volume overload (AVO), resulting in cardiac failure and increased cardiac oxygen consumption (1). There is increasing awareness of the prognostic significance of right-sided heart congestion during AVO and acute cardiac failure (2). Low coronary perfusion pressure associated with acute right-sided heart congestion leads to cardiac remodeling triggered by myocardial oxygen deprivation generating reactive oxygen species (ROS) (3). Developing myocardial pressure due to ventricle volume overload may cause progressive myocardial ischemia (4).

Myocardial ischemia is associated with an increase in ROS production originating from several enzyme systems, such as oxidases of nicotinamide adenine dinucleotide phosphatase (NADPH), xanthine oxidase, electron leakage from the mitochondrial respiratory chain, cyclooxygenases, and uncoupled endothelial nitric oxide synthase. Among these, monoamine oxidases (MAOs) have recently been under intense investigation and may contribute to vascular dysfunction after volume overload (5). MAOs are located in the outer mitochondrial membrane and have been shown to act against the arterial wall during ischemia by generating ROS during the oxidative breakdown of key neurotransmitters, such as norepinephrine, epinephrine, and dopamine (6). Mitochondrial MAOs are flavoproteins that exist in two isoforms (MAO-A and MAO-B) that are involved in the metabolism of biogenic amines in vascular cells during oxidative stress and are distinguished by different substrate specificities and inhibitor sensitivities (6, 7). MAO-A activates the sphingolipid pathway (7), and MAO inhibitors may have therapeutic potential in myocardial hypertrophy and cardiac failure (8, 9). Among a few other research groups, we have previously shown that moclobemide (Mo), an MAO-A inhibitor, ameliorates recovery after ischemia (10).

Address for correspondence: Ari Mennander, MD, Tampere University Heart Hospital, Cardiac Research and Tampere University; Ensitie 4, Tampere 33520 2000 Tampere-*Finland*
Phone: +358 3 31164945 E-mail: ari.mennander@hotmail.com
Accepted Date: 01.10.2018 **Available Online Date:** 13.12.2018

DOI:10.14744/AnatolJCardiol.2018.37336

Anatol J Cardiol 2019; 21: 39-45
DOI:10.14744/AnatolJCardiol.2018.37336

We hypothesized that Mo impacts the myocardial arteries early after AVO in a rat model simulating the clinical scenario of acute cardiac insufficiency by performing a surgical 5 mm long abdominal aortocaval fistula. The aim of the present study was to investigate the effect of Mo on acute myocardial changes after experimental AVO with the aid of chitinase 3-like protein (YKL-40) that interacts with cell proliferation, differentiation, inflammation, and remodeling of the extracellular matrix and inhibits apoptosis (11). To demonstrate the validity of our model, atrial natriuretic peptide (ANP) and brain natriuretic peptide (BNP) were investigated; these cardiac hormones represent compensation of congestive heart failure due to their vasodilating, antiproliferative, and neurohumoral-modulating capacities (12). Myocardial inflammation and remodeling was analyzed with hypoxia-inducible factor 1-alpha (HIF1α) (13), inducible nitric oxide synthase (iNOS), interleukin 6 (IL-6), E-selectin, vascular endothelial growth factor-alpha (VEGFα), matrix metalloproteinase 9 (MMP9), CD68 for macrophages, and transforming growth factor-beta (TGFβ).

Methods

Rats

Sixty Fischer 344 rats (F344/NHsd; Harlan Laboratories, The Netherlands) weighing 200–350 g underwent surgical abdominal arterial–venous fistula to induce AVO, with six normal hearts from non-operated rats serving as controls. The rats were kept in the University of Tampere vivarium and received humane care in compliance with the "Principles of Laboratory Animal Care" formulated by the National Society for Medical Research and the "Guide for the Care and Use of Laboratory Animals" prepared by the Institute of Laboratory Animal Resources and published by the National Institutes of Health (publication no. 86-23, revised 1996). The study was approved by the Finnish State Provincial Office.

Surgical procedure

Rats were anesthetized with sevoflurane (Baxter, USA) for inhalation and pentobarbiturate (50 mg/kg, Mebunat vet®; Orion, Espoo, Finland) intraperitoneally. The abdominal cavity was surgically opened, and the inferior vena cava and the aorta were exposed. An arterio-venous fistula was performed intra-abdominally by incising vertically 5 mm both the abdominal aorta and the adjacent inferior vena cava and joining these vessels surgically with a 7-0 running vascular suture. After surgery, 100 U Heparin Leo (Vianex S.A., Greece) was administered intravenously. From the abdominal aorta, oxygenated blood was introduced into the abdominal vena cava, thus resulting in AVO of the heart. The surgical procedure was confirmed by observing the immediate inferior vena cava circulating blood color change from dark blue to pale blue proximal to the created arterio-venous fistula. The pulsation of arterial blood was both visualized and palpated on the inferior vena cava proximal adjacent to the fistula. This model allowed the study of extensive AVO and associated myocardial changes *in vivo*. The model thus simulated the clinical concept of volume overload without ischemia (14). After the procedure, buprenorphine (0.1 mg/100 g, Vetergesic®; Orion) and carprofen (0.5 mg/100 g, Norocarp®; Norbrook Laboratories Limited, Newry, Northern Ireland) were given subcutaneously for pain relief. Sixty syngeneic Fischer rats underwent surgical abdominal aortocaval fistula to induce AVO. Among these, 18 rats were treated with Mo 10 mg/kg/day by subcutaneous injection (AVO+Mo), and 42 rats with AVO were left untreated for comparison.

Tissue samples

The rats were sacrificed 1 (n=32) or 3 (n=16) days after AVO, whereas 12 rats were lost due to acute cardiac failure. Six normal hearts from non-operated rats were also obtained. The basal part of the hearts was separated and stored in RNA later (Applied Biosystems, CA, USA) for quantitative reverse transcription polymerase chain reaction (RT-PCR) analysis. The apex part of the heart was fixed in formalin and embedded in paraffin.

Histology

For histology, 5 μm sections were cut and stained with hematoxylin and eosin. The presence of subendocardial and myocardial edema, hemorrhage, and ischemia was evaluated from all samples. As the vacuolization of the nuclei in the medial layer of the intramyocardial arteries reflects edema, a representative cross-sectional intramyocardial artery was selected randomly from both the left anterior, septum, and right posterior ventricular walls. Normal, edematous, and sharp-edged medial cell nuclei were manually counted separately. The relative number of ischemic nuclei of intramyocardial arteries was calculated by dividing the total number of sharp-edged medial cell nuclei by the normal round-shaped nuclei. The presence of periadventitial inflammatory cells was graded according to an arbitrary scale from 0 to 1, with 0, no inflammation and 1, presence of inflammation. The evaluation of the histology was performed by two investigators blinded to the study protocol.

Immunohistochemistry

Immunohistochemistry was performed to three untreated controls and three hearts after AVO with Mo using Ventana Lifesciences Benchmark XT© Staining module. The paraffin-embedded slides were deparaffinized with three changes of xylene, rehydrated in a series of graded ethanol, and rinsed well under running distilled water. The slides were placed in a preheated retrieval buffer, 0.1 mmol EDTA, pH 8.0, for 30 min and then cooled in a buffer for 5 min, followed by a 5-minute rinse under running distilled water. After heat-induced epitope retrieval, the slides were placed on an autostainer (DAKO Corp., Carpinteria, CA, USA). Sections were incubated with 3% hydrogen peroxide in ethanol for 5 min to inactivate the endogenous peroxides and incubated in CD68 antibody (dilution 1:100) (Biomedica Gruppe, Germany) or YKL-40 antibody (dilution 1:100) (Biomedica Gruppe) for 30 min, followed by rinsing with Tris-buffered saline solution with Tween 20 (TBST)

wash buffer. Secondary incubation was made using DUAL-labeled polymer horseradish peroxidase (K4061; DAKO Corp.) for 15 min. The slides were rinsed with TBST wash buffer. Sections were then incubated in 3,3′-diaminobenzidine (K3467; DAKO Corp.) for 5 min, counterstained with modified Schmidt hematoxylin for 5 min, rinsed for 3 min in tap water to blue sections, dehydrated with graded alcohols, and cleared in three changes of xylene before mounting. Positively stained CD68 and YKL-40 depositions were evaluated from a representative cross-sectional intramyocardial artery selected randomly from the left anterior ventricular wall, right ventricular wall, and septum. The evaluation was performed by two investigators blinded to the study protocol.

Quantitative RT-PCR analysis

The frozen tissue of the base of the heart of six randomly selected hearts from each group was homogenized, and RNA extraction was performed using GenElute™ Mammalian Total RNA Miniprep kit (Sigma-Aldrich, St. Louis, MO, USA) with proteinase K treatment. Total RNA was then reverse-transcribed to cDNA using TaqMan® Reverse Transcription reagents and random hexamers (Applied Biosystems). The cDNA obtained from the RT reaction (amount corresponding to approximately 1 ng of total RNA) was subjected to quantitative PCR using QuantiTect® Primer Assays (Qiagen, Valencia, CA, USA) for ANP, MMP9, TGFβ, YKL-40, BNP, iNOS, IL-6, VEGFα, and glyceraldehyde 3-phosphate dehydrogenase (GAPDH); Maxima® SYBR Green/ROX qPCR Master Mix (Thermo Fisher Scientific, Waltham, MA, USA); and ABI PRISM 7000 Sequence detection system (Applied Biosystems). The PCR reaction parameters for SYBR® Green detection were as follows: incubation at 50 °C for 2 min and 95 °C for 10 min, 40 cycles of denaturation at 95 °C for 15 s, and annealing and extension at 60 °C for 1 min. Each sample was determined in duplicate. The Ct values were determined, and the relative quantification was calculated using the $2^{-\Delta\Delta Ct}$ method (15). The values of six control samples were used as a calibrator, and the expression levels of HIF1α, ANP, BNP, iNOS, IL-6, VEGFα, MMP9, TGFβ, and YKL-40 were normalized against GAPDH.

Statistical analysis

Data are presented as median (Q1-Q3). Statistical analyses were performed using the SPSS 22.0 statistical software (SPSS Inc., Chicago, IL, USA). For multiple comparison, data between the groups were analyzed using the Kruskal-Wallis test and confirmed using the Mann-Whitney U test, when appropriate. A p-value <0.05 was considered significant.

Results

Histology

The presence of subendocardial and myocardial edema, hemorrhage, myocardial inflammation and ischemia of the ventricles did not differ in the hearts with AVO+Mo as compared with AVO. After 1 day, the absolute number of normal nuclei of intramyocardial arteries in the right ventricle was higher in AVO+Mo than in AVO and controls [60.00 (32.25–95.50) vs. 32.50 (21.25–38.50) and 28.50 (24.50–34.75), point score unit (PSU), p=0.008, Table 1]. After 3 days, the absolute number of ischemic

Table 1. Histology of medial cell nuclei of intramyocardial arteries of the hearts with AVO after 1 and 3 days compared with AVO+Mo

		Day 1			Day 3		
	Controls	AVO	AVO+Mo	*P*-value	AVO	AVO+Mo	*P*-value
Right ventricle							
Normal nuclei	28.50 (24.50-34.75)	32.50 (21.25-38.50)	60.00 (32.25-95.50)	0.008*	38.00 (31.00-40.00)	44.00 (36.25-77.00)	0.385
Ischemic nuclei	1 (0-3.50)	2.50 (1.00-4.00)	2.00 (1.25-7.50)	0.808	3.00 (1.00-5.00)	1.50 (1.00-6.25)	0.636
Edematous nuclei	2.00 (0.75--6.25)	3.00 (1.00-5.75)	2.50 (1.00-5.50)	0.826	0 (0-2.00)	3.00 (0.25-7.00)	0.038*
Left ventricle							
Normal nuclei	46.00 (30.00-66.25)	45.00 (36.00-63.00)	58.00 (48.75-71.75)	0.074	53.00 (51.00-69.00)	42.00 (33.25-61.25)	0.115
Ischemic nuclei	2.00 (1.00-2.00)	3.00 (2.00-5.00)	4.00 (2.00-8.00)	0.478	5.00 (3.25-9.00)	2.00 (1.00-4.50)	0.026*
Edematous nuclei	4.00 (0.75--10.00)	2.00 (0-5.00)	1.50 (1.00-4.50)	0.732	0.50 (0-1.00)	1.00 (0.25-3.25)	0.259
Septum							
Normal nuclei	31.00 (19.25-44.25)	39.00 (24.00-50.00)	36.00 (22.00-46.00)	0.885	39.00 (28.25-48.25)	36.00 (22.00-43.00)	0.668
Ischemic nuclei	1.00 (0-2.25)	3.50 (2.00-7.00)	5.00 (3.00-6.00)	0.635	5.00 (3.00-7.50)	3.00 (2.00-4.00)	0.128
Edematous nuclei	3.00 (0-5.75)	4.00 (2.00-8.00)	3.00 (3.00-6.00)	0.747	0.50 (0-1.25)	3.00 (2.00-10.00)	0.009*

Values are expressed as median (Q1–Q3). Results of multiple comparison including Kruskal–Wallis test confirmed with Mann–Whitney U test, when appropriate. Differences with a *P*-value <0.05 were considered significant.
AVO - acute volume overload; Mo - moclobemide

Anatol J Cardiol 2019; 21: 39-45
DOI:10.14744/AnatolJCardiol.2018.37336

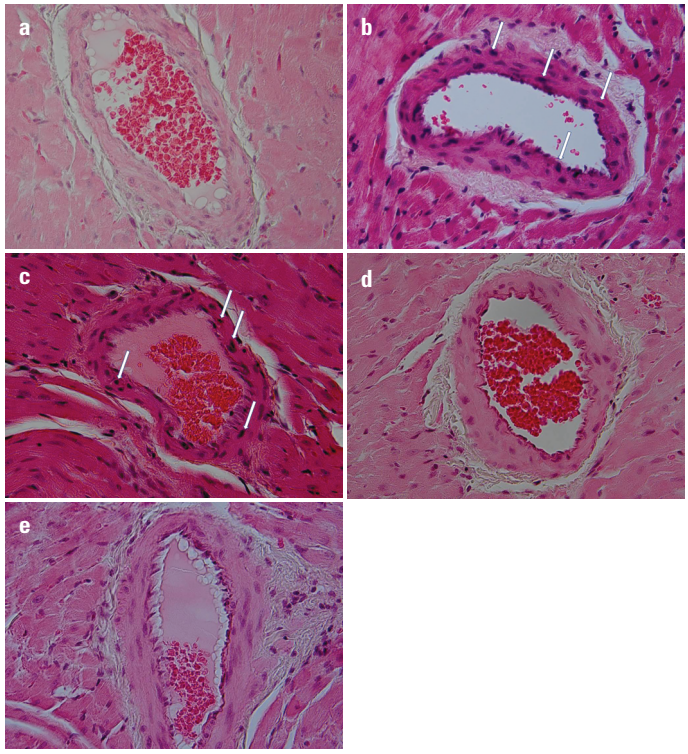

Figure 1. Representative histology of a septal intramyocardial artery of a normal heart (a; control), hearts with acute volume overload 1 day (b; AVO 1 day) and 3 days (c; AVO 3 days) after surgery, and hearts with acute volume overload and moclobemide 1 day (d; AVO+Mo 1 day) and 3 days (e; AVO+Mo 3 days) after surgery (×40 magnification). Note the increased dark ischemic nuclei of the media in B and C (arrows)

nuclei of intramyocardial arteries in the left ventricle was lower in AVO+Mo than in AVO and controls [2.00 (1.00–4.50) vs. 5.00 (3.25–9.00) and 2.00 (1.00–2.00), PSU, p=0.026, Fig. 1], and the relative number of ischemic nuclei of intramyocardial arteries in the left ventricle was lower in AVO+Mo than in AVO [0.04 (0.02–0.07) vs. 0.09 (0.07–0.14), PSU, p=0.036, Fig. 2]. The presence of edematous nuclei of myocardial arteries in the right ventricle and septum was higher in AVO+Mo than in AVO and controls [3.00 (0.25–7.00) vs. 0 (0–2.00) and 2.00 (0.75–6.25), PSU, p=0.038 and 3.00 (2.00–10.00) vs. 0.50 (0–1.25) and 3.00 (0–5.75), PSU, p=0.009]. The relative number of edematous nuclei of myocardial arteries in the right ventricle and septum was higher in AVO+Mo than in AVO [0.07 (0.01–0.12) vs. 0 (0–0.05), PSU, p=0.038 and 0.18 (0.03–0.23) vs. 0.02 (0–0.03), PSU, p=0.010].

Immunohistochemistry

CD68 and YKL-40 were equally distributed in both AVO and AVO+Mo (Fig. 3).

Quantitative RT-PCR analysis

ANP was lower after 1 day in AVO+Mo than in AVO and controls [0.95 (0.37–1.84) vs. 2.40 (1.33–3.09) and 0.96 (0.38–9.6), FC, p=0.044, Table 2], whereas YKL-40 was higher after 1 and 3 days in AVO+Mo than in AVO and controls [22.66 (14.05–28.83) vs. 10.06

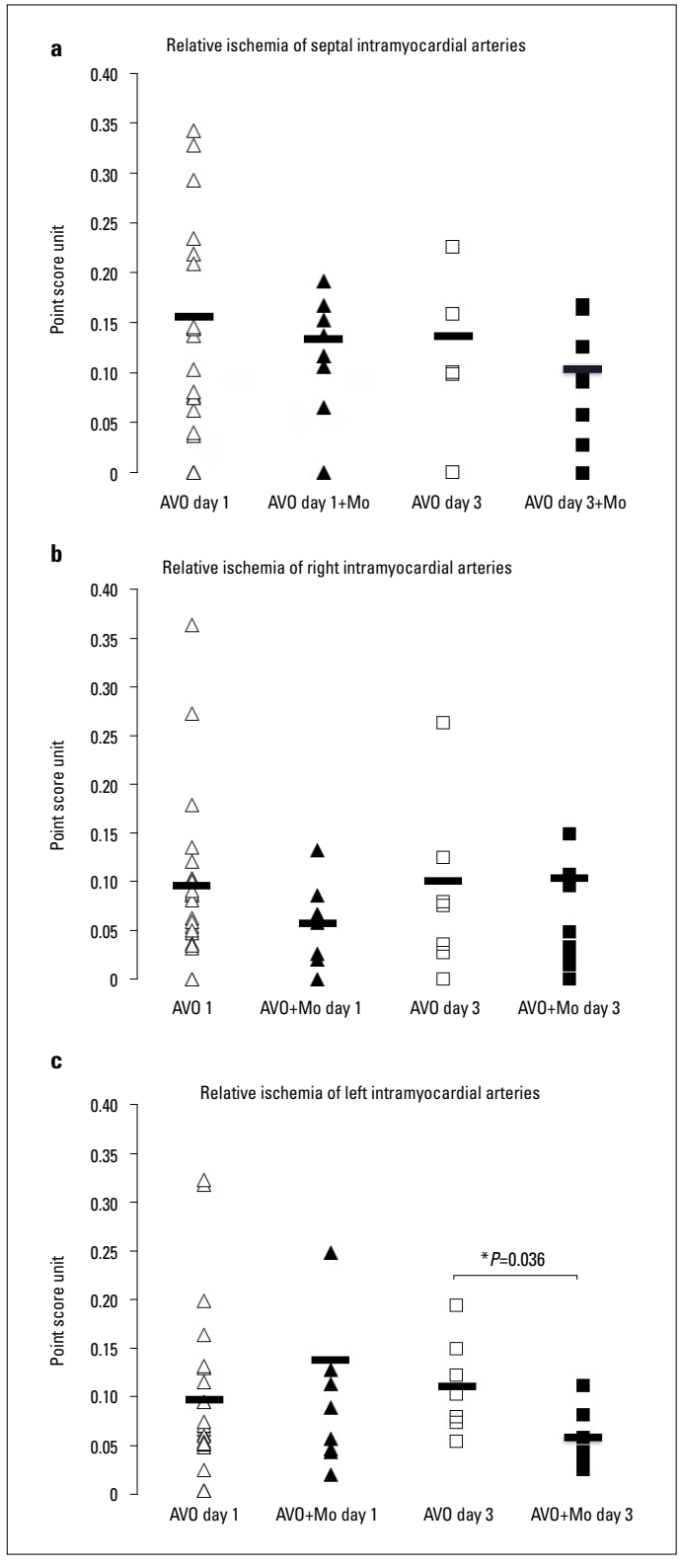

Figure 2. Relative ischemia of intramyocardial arteries of the septum (a), right ventricle (b), and left ventricle (c) of the hearts with acute volume overload 1 day (AVO 1 day, white triangles), treated with moclobemide (AVO+Mo 1 day, black triangles), hearts with acute volume overload 3 days (AVO 3 days, white squares), and treated with moclobemide (AVO+Mo 3 days, black squares). *P<0.05, Mann-Whitney. Horizontal bars indicate the mean

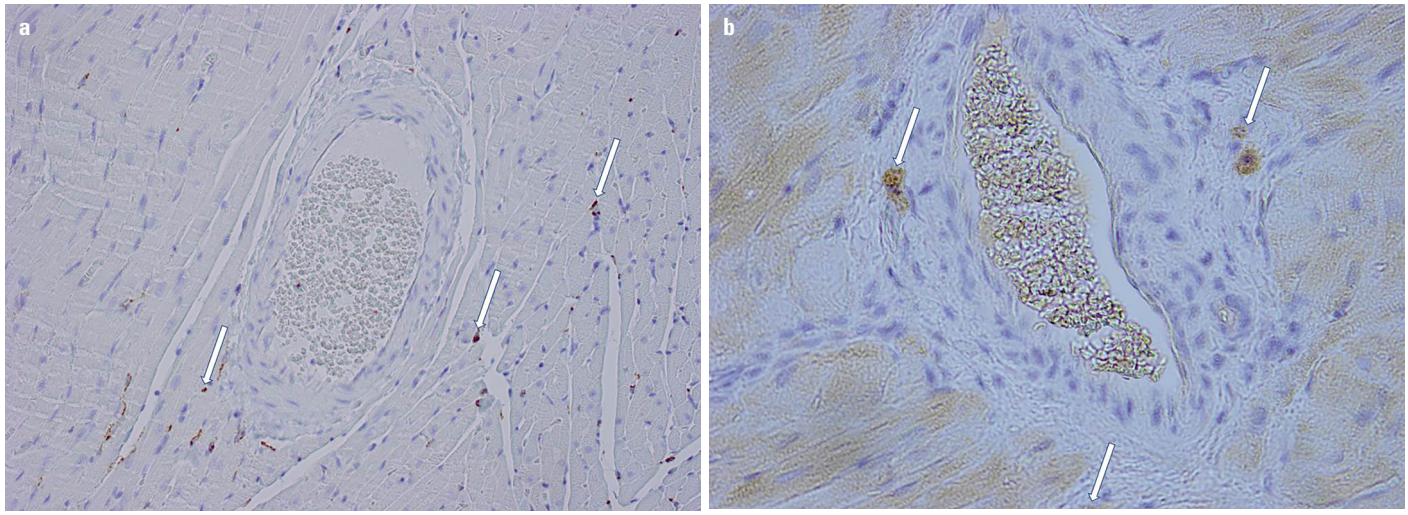

Figure 3. Representative immunohistochemistry for CD68 deposition (a) and YKL-40 (b) in the hearts with acute volume overload and moclobemide 3 days after surgery (×40 magnification). Arrows show positive staining

Table 2. Gene expression of the hearts with AVO+Mo at 1 and 3 days compared with AVO

		Day 1			Day 3		
	Controls	AVO	AVO+Mo	*P*-value	AVO	AVO+Mo	*P*-value
HIF1α	0.92 (0.84-1.04)	1.29 (0.77-1.82)	1.51 (1.22-2.00)	0.574	1.25 (1.02-1.41)	1.30 (1.07-1.44)	0.600
iNOS	0.82 (0.28-1.31)	1.20 (0.73-5.00)	1.01 (0.62-2.34)	0.336	0.96 (0.52-0.96)	0.70 (0.56-1.15)	0.749
E-selectin	0.97 (0.59-1.62)	2.90 (2.12-6.12)	4.19 (3.75-6.55)	0.193	1.64 (1.36-2.88)	3.31 (2.56-3.88)	0.079
ANP	0.96 (0.38-9.6)	2.40 (1.33-3.09)	0.95 (0.37-1.84)	0.044*	1.38 (0.97-2.93)	1.27 (0.88-1.38)	0.418
BNP	1.03 (1.01-1.11)	0.97 (0.38-3.25)	0.63 (0.40-1.65)	0.335	0.68 (0.58-0.98)	0.65 (0.43-1.09)	0.908
VEGFα	0.90 (0.81-1.00)	0.61 (0.34-0.88)	0.65 (0.47-0.82)	0.821	1.31 (0.80-1.68)	1.48 (1.33-1.65)	0.462
MMP9	0.69 (0.37-1.77)	9.02 (2.62-15.54)	10.55 (3.58-15.19)	0.914	4.76 (3.63-7.88)	9,68 (5.12-11.41)	0.200
YKL-40	0.75 (0.58-0.98)	10.06 (6.23-15.02)	22.66 (14.05-28.83)	0.006*	3.70 (2.62-5.35)	6.03 (4.72-7.18)	0.025*
TGFβ	1.01 (0.70-1.26)	1.90 (3.76-5.12)	3.62 (3.03-4.72)	0.792	2.69 (2.23-3.89)	3.82 (2.61-5.20)	0.121

Values are expressed as median (Q1–Q3). Results of multiple comparison including Kruskal–Wallis test confirmed with Mann–Whitney U test, when appropriate. Differences with a *P*-value <0.05 were considered significant.
AVO - acute volume overload; Mo - moclobemide; HIF1α - hypoxia-inducible factor 1-alpha; iNOS - inducible nitric oxide synthase; ANP - atrial natriuretic peptide; BNP - brain natriuretic peptide; VEGFα - vascular endothelial growth factor-alpha; MMP9 - matrix metalloproteinase 9; YKL-40 - chitinase 3-like protein; TGFβ - tumor growth factor β

(6.23–15.02) and 0.75 (0.58–0.98), FC, p=0.006 and 6.03 (4.72–7.18) vs. 3.70 (2.62–5.35) and 0.75 (0.58–0.98), FC, p=0.025].

Discussion

In the present study, Mo decreased the number of ischemic nuclei of intramyocardial arteries of the left ventricle while preserving the number of normal and edematous nuclei of the right ventricle and septum after AVO.

We separately investigated the histology of three different compartments of the heart to demonstrate the interactive connection between the ventricles during AVO. In this model, AVO leads to a dramatic burst of blood to the right side of the heart, pushing the septum toward the left side of the heart at day 3, thus inducing ischemia of intramyocardial arteries along with cellular swelling of the left ventricle. The whole of the heart eventually results in early myocardial remodeling associated with ischemia and release of ROS. The generated ROS are responsible for many signaling responses, including activation of tyrosine kinase receptors, sphingolipid pathway, transcription factors, and activation of proapoptotic pathways with caspase activation and calcium deregulation, among others (6). Among these, oxidation of biogenic amines by MAO may at least partly influence the association of ROS and ischemia with the trigger of alteration of myocardial arteries (6). The development of subsequent cardiac hypertrophy is associated with the presence of MAO and hydrogen peroxidase production by oxidative stress (9).

Anatol J Cardiol 2019; 21: 39-45
DOI:10.14744/AnatolJCardiol.2018.37336

The generation of ROS is associated with the sphingolipid pathway that may mediate the association of MAO with AVO. The mitochondrial MAO-A metabolizes serotonin, which is released by activated platelets during AVO. Vascular smooth muscle cell proliferation is dependent on serotonin metabolism (16) and MAO (17). The target of MAO inhibition is the mitochondria that react upon AVO; selective MAO inhibition blocks the release of hydrogen peroxide and concomitant production of detrimental ROS (18). Edematous nuclei of intramyocardial arteries of the right ventricle and septum are preserved with concomitant decrease of ischemic nuclei of the left ventricle during Mo. Thus far at day 1, Mo increased the number of normal nuclei of intramyocardial arteries, suggesting the preservation of cellular integrity.

Of note, Mo did not impact on inflammation during the early phase of AVO; periadventitial inflammation of intramyocardial arteries was even undetected. There were no differences in the expressions of inflammatory parameters, such as E-selectin, MMP9, TGFβ, and VEGFα, in the hearts treated with Mo as compared with the controls. All hearts with AVO showed positive immunohistochemical staining for CD68 and YKL-40. However, the tissue expression of YKL-40 was higher, while ANP was lower in the hearts with AVO+Mo than in those with untreated AVO. Instead of interacting with inflammation per se, Mo may regulate the inflammatory macrophages toward the M2 phenotype that has a strong remodeling capacity.

An increased serum YKL-40 may indicate excessive cleavage of the glycoprotein-like molecule on the endothelium of the intramyocardial arteries, suggesting an increased activation of proinflammatory and profibrotic cytokines after ischemia (19). Alternately, the expression of tissue YKL-40 is a sign of tissue remodeling after ischemia (20-22). YKL-40 has an angiogenic property that may preserve the cells from apoptosis and cell death (23). It inhibits inflammation and cell apoptosis by decreasing Fas expression, activating protein kinase B/protein kinase B, and inducing Faim 3 (20). It regulates the intensity of T helper cell 2 (Th2)-dominated diseases while increases the accumulation of T cells and alternatively activates M2 macrophages (20). Interestingly, the Th2 cytokines, IL-4 and IL-13, also polarize macrophages toward the YKL-40-producing M2 phenotype macrophages (24).

Nevertheless, the exact mechanisms associated with MAO-A inhibition during AVO remain to be elucidated. The selected gene expressions reflected the overall outcome after AVO. Previously, the activation of the mitochondrial electron transport chain, NADPH oxidase, and xanthine oxidase has been speculated to increase during ROS generation after AVO. However, ischemia may occur in the organs known to be deficient for xanthine oxidase and in a mouse model without a functional NADPH oxidase (18). The sphingolipid pathway seems therefore plausible in our model; MAO regulates through ROS the lipid peroxidation of cell membranes, protein and enzyme oxidation, and some irreversible DNA changes leading to cell death (18). In a recent experimental study by Sturza et al. (5), MAOs are shown to be responsible for vascular damage by decreasing peroxidation and endothelial nitric oxide release.

Study limitations

The limitations of the present study include the plausible interaction with catecholamine metabolism due to MAO inhibition (25). We therefore chose Mo, a selective and reversible MAO inhibitor. The reversibility of MAO inhibition may abolish the possible side effects due to catecholamine metabolism. In addition, cardioprotection may be induced via autophagy after myocardial damage, and inducing autophagy sequestration may lead to novel therapeutic options against myocardial ischemia (26). Future investigation of plasma parameters for myocardial damage and oxidative stress is recommended. We did not measure the left ventricular ejection fraction to describe cardiac function. AVO includes a dispersed range of histological findings necessitating the careful statistical interpretation of the results. The results should be cautiously interpreted; the findings and conclusions should not be simply translated to humans in the real clinical setting.

Conclusion

In conclusion, MAO may be associated with AVO. We suggest further studies of MAO inhibition after AVO. Despite these promising experimental results, clinical studies will be necessary to evaluate the therapeutic properties of MAO inhibitors after AVO, especially in the organs, such as the heart, containing a large amount of MAOs.

Conflict of interest: None declared.

Peer-review: Externally peer-reviewed.

Authorship contributions: Concept – A.M; Design – M.H., T.P., A.M.; Supervision – T.P., E.M., A.M.; Fundings – T.P., E.M., A.M.; Materials – T.P., E.M., A.M.; Data collection &/or processing – C.H., M.H., A.M.; Analysis &/or interpretation – C.H., M.H., T.P., E.M., A.M.; Literature search – C.H., E.M., A.M.; Writing – C.H., E.M., A.M.; Critical review – C.H., M.H., T.P., E.M., A.M.

References

1. Harjola VP, Mebazaa A, Celutkiene J, Bettex D, Bueno H, Chioncel O, et al. Contemporary management of acute right ventricular failure: a statement from the Heart Failure Association and the Working Group on Pulmonary Circulation and Right Ventricular Function of the European Society of Cardiology. Eur J Heart Fail 2016; 18: 226-41.
2. Generali T, Garatti A, Biondi A, Varrica A, Menicanti L. Aorta to right atrial shunt due to the rupture of a degenerative aneurysm of the noncoronary sinus of Valsalva. J Cardiovasc Med (Hagerstown) 2013; 14: 71-3. [CrossRef]

3. Mazzo FR, de Carvalho Frimm C, Moretti AI, Guido MC, Koike MK. Acute aortocaval fistula: role of low perfusion pressure and subendocardial remodeling on left ventricular function. Int J Exp Pathol 2013; 94: 178-87. [CrossRef]
4. Aronson D, Darawsha W, Atamna A, Kaplan M, Makhoul BF, Mutlak D, et al. Pulmonary hypertension, right ventricular function, and clinical outcome in acute decompensated heart failure. J Card Fail 2013; 19: 665-71. [CrossRef]
5. Sturza A, Leisegang MS, Babelova A, Schröder K, Benkhoff S, Loot AE, et al. Monoamine oxidases are mediators of endothelial dysfunction in the mouse aorta. Hypertension 2013; 62: 140-6. [CrossRef]
6. Coatrieux C, Sanson M, Negre-Salvayre A, Parini A, Hannun Y, Itohara S, et al. MAO-A induced mitogenic signaling is mediated by reactive oxygen species, MMP-2, and the shingolipid pathway. Free Radic Biol Med 2007; 43: 80-9. [CrossRef]
7. Pchejetski D, Kunduzova O, Dayon A, Calise D, Seguelas MH, Leducq N, et al. Oxidative stress-dependent spingosine kinase-1 inhibition mediates monoamine oxidase A-associated cardiac cell apoptosis. Circ Res 2007; 100: 41-9. [CrossRef]
8. Bianchi P, Kunduzova O, Masini E, Cambon C, Bani D, Raimondi L, et al. Oxidative stress by monoamine oxidase mediates receptor-independent cardiomyocyte apoptosis by serotonin and postischemic myocardial injury. Circulation 2005; 112: 3297-305. [CrossRef]
9. Bianchi P, Pimentel DR, Murphy MP, Colucci WS, Parini A. A new hypertrophic mechanism of serotonin in cardiac myocytes: receptorindependent ROS generation. FASEB J 2005; 19: 641-3. [CrossRef]
10. Vuohelainen V, Hämäläinen M, Paavonen T, Karlsson S, Moilanen E, Mennander A. Inhibition of monoamine oxidase A increases recovery after experimental cardiac arrest. Interact Cardiovasc Thorac Surg 2015; 21: 441-9. [CrossRef]
11. Tiriveedhi V, Upadhya GA, Busch RA, Gunter KL, Dines JN, Knolhoff BL, et al. Protective role of bortezomib in steatotic liver ischemia/reperfusion injury through abrogation of MMP activation and YKL-40 expression. Transpl Immunol 2014; 30: 93-8. [CrossRef]
12. Stumpe KO, Sölle H, Klein H, Krück F. Mechanism of sodium and water retention in rats with experimental heart failure. Kidney Int 1973; 4: 309-17. [CrossRef]
13. Anan M, Abe T, Matsuda T, Ishii K, Kamida T, Fujiki M, et al. Induced angiogenesis under cerebral ischemia by cyclooxygenase 2 and hypoxia-inducible factor naked DNA in a rat indirect bypass model. Neurosci Lett 2006; 409: 118-23. [CrossRef]
14. Huuskonen C, Hämäläinen M, Bolkart R, Soininen T, Kähönen V, Paavonen T, et al. Surgical acute volume-overload impacts early on myocardium- an experimental study. Acta Cardiol Sin 2017; 33: 630-6.
15. Livak KJ, Schmittgen TD. Analysis of relative gene expression data using real-time quantitative PCR and the 2-ΔΔCt method. Methods 2001; 25: 402-8. [CrossRef]
16. Day RM, Agyeman AS, Segel MJ, Chévere RD, Angelosanto JM, Suzuki YJ, et al. Serotonin induces pulmonary artery smooth muscle cell migration. Biochem Pharmacol 2006; 71: 386-97. [CrossRef]
17. Liu Y, Wei L, Laskin DL, Fanburg BL. Role of protein transamidation in serotonin-induced proliferation and migration of pulmonary artery smooth muscle cells. Am J Respir Cell Mol Biol 2011; 44: 548-55. [CrossRef]
18. Kunduzova OR, Bianchi P, Pizzinat N, Escourrou G, Seguelas MH, Parini A, et al. Regulation of JNK/ERK activation, cell apoptosis, and tissue regeneration by monoamine oxidases after renal ischemia-reperfusion. FASEB J 2002; 16: 1129–31. [CrossRef]
19. Mathiasen AB, Harutyunyan MJ, Jørgensen E, Helqvist S, Ripa R, Gøtze JP, et al. Plasma YKL-40 in relation to the degree of coronary artery disease in patients with stable ischemic heart disease. Scan J Clin Lab Invest 2011; 71: 439-47. [CrossRef]
20. Lee CG, Hartl D, Lee GR, Koller B, Matsuura H, Da Silva CA, et al. Role of breast regression protein 39 (BRP-39)/chitinase 3-like-1 in Th2 and IL-13–induced tissue responses and apoptosis. J Exp Med 2009; 206: 1149-66. [CrossRef]
21. Mathiasen AB, Harutyunyan MJ, Jørgensen E, Helqvist S, Ripa R, Gøtze JP, et al. Plasma YKL-40 in relation to the degree of coronary artery disease in patients with stable ischemic heart disease. Scand J Clin Lab Invest 2011; 71: 439-47. [CrossRef]
22. Tiriveedhi V, Upadhya GA, Busch RA, Gunter KL, Dines JN, Knolhoff BL, et al. Protective role of bortezomib in steatotic liver ischemia/reperfusion injury through abrogation of MMP activation and YKL-40 expression. Transpl Immunol 2014; 30: 93-8. [CrossRef]
23. Faibish M, Francescone R, Bentley B, Yan W, Shao R. A YKL-40-neutralizing antibody blocks tumor angiogenesis and progression: a potential therapeutic agent in cancers. Mol Cancer Ther 2011; 10: 742-51. [CrossRef]
24. Murray PJ, Wynn TA. Protective and pathogenic functions of macrophage subsets. Nat Rev Immunol 2011; 11: 723-37. [CrossRef]
25. Kaludercic N, Takimoto E, Nagayama T, Feng N, Lai EW, Bedja D, et al. Monoamine oxidase A-mediated enhanced catabolism of norepinephrine contributes to adverse remodeling and pump failure in hearts with pressure overload. Circ Res 2010; 106: 193–202. [CrossRef]
26. Wu X, He L, Cai Y, Zhang G, He Y, Zhang Z, et al. Induction of autophagy contributes to the myocardial protection of valsartan against ischemia reperfusion injury. Mol Med Rep 2013; 8: 1824-30. [CrossRef]